Chapter-5

Structural, Chemical & Optical studies of Few layer Graphene Oxide (FLGO) and reduced Graphene Oxide-Zinc Oxide (rGO-ZnO) heterostructures

5.1 Synthesis methodology

- **Synthesis of Graphene Oxide:**

Graphene oxide was synthesized via modified Hummers method [18] by oxidation of inexpensive graphite precursor with strong oxidising agents such as sulphuric acid and potassium permanganate with sodium nitrate as the catalyst. Ultrasonication technique was combined with modified Hummers method to reduce the long duration of oxidation step and to decrease the no. of layers in as synthesized graphene oxide. The proposed sonochemical method could simultaneously decrease the reaction temperature and production time and result in few layer GO. The obtained precipitate was purified by multiple rinsing via centrifugation successively with 10% HCl, DI water and absolute ethanol. Final purified product was dried at 60°C for 24 hr in a vaccum oven and stored in a desiccator for further characterization.

- **Synthesis of Reduced Graphene Oxide/ ZnO heterostructures:**

Solvothermal synthesis was utilized to prepare hybrid rGO_ZnO heterostructure. Firstly, GO powder was dispersed by ultrasonication for 4hr in DI water. Separately zinc acetate dihydrate was stirred in a 1:1 mixture of DI:Ethanol until dissolved. The molar ratio of GO to ZnO was kept 1:3. After complete dissolution of ZAD, 0.1M NaOH solution was slowly added dropwise and allowed to stir. The zinc oxide precursor solution was then slowly added to the GO solution and stirred for another 2 hrs for homogenous mixing. The final solution was transferred to a Teflon lined hydrothermal autoclave and the reaction was kept at 120°C for 24 hr. The precipitate was filtered, purified and dried using the exact same protocol as mentioned above for Graphene Oxide and stored in a desiccator for further characterization.

5.2 Experimental methods

XRD- Crystallographic studies of GO nanosheets and rGO_ZnO heterostructures were carried out on Rigaku Miniflex-600 equipped with Cu-Kα radiation and graphite monochromator. The diffraction angle was utilized to calculate the interlayer spacing of the exfoliated Graphene oxide nanosheets.

HRTEM- Size, morphology and crystalline nature of nanosheets and heterostructures were studied using a Tecnai G2 20 Twin High resolution Transverse Electron Microscope by FEI USA. An extremely low concentration DMF dispersion was drop cast on a carbon-coated copper grid and was dried in a vacuum oven at 60ºC for one hour before analysis.

FESEM- Microstructural investigation of nanomaterial's surface was performed with Sigma 300 Field Emission Scanning Electron Microscope by Zeiss. The sample was sputtered with a thin conductive layer of gold prior to imaging to avoid charging of the sample by electron beam. Data was acquired varying the accelerating voltage between 5 and 15 kV.

FTIR- The Fourier transform infrared spectra was collected in the range 400-4000 nm using Nicolet iS5 spectrometer by THERMO Electron Scientific Instruments LLC. ATR mode was utilized for the characterization.

Raman- Raman spectroscopy was also performed in the range of 400-4000 nm using Witec alpha300 RAS (made in Germany).

AFM- Surface topography and sheet thickness were obtained using Park XE7 (South Korea) Atomic Force Microscope operated in contact mode. Cross-sectional profile was acquired from the AFM data with the help of Gwyddion software.

UV-Vis Spectroscopy- The UV-Vis absorption spectra was recorded on dilute ethanol suspension with pure ethanol as reference using BioSpectrometer kinetic by Eppendorf and was used to calculate the band gap energy of GO nanosheets and rGO_ZnO heterostructures.

PLE- Photoluminescence emission spectra of GO nanosheets and rGO_ZnO heterostructures was acquired in the wavelength range 400-800 nm using Fluorescence Spectrophotometer F-4600 by Hitachi with excitation and emission slit width 5 nm and PMT voltage 700 V.

5.3 Results & Discussion

5.3.1 Structural analysis

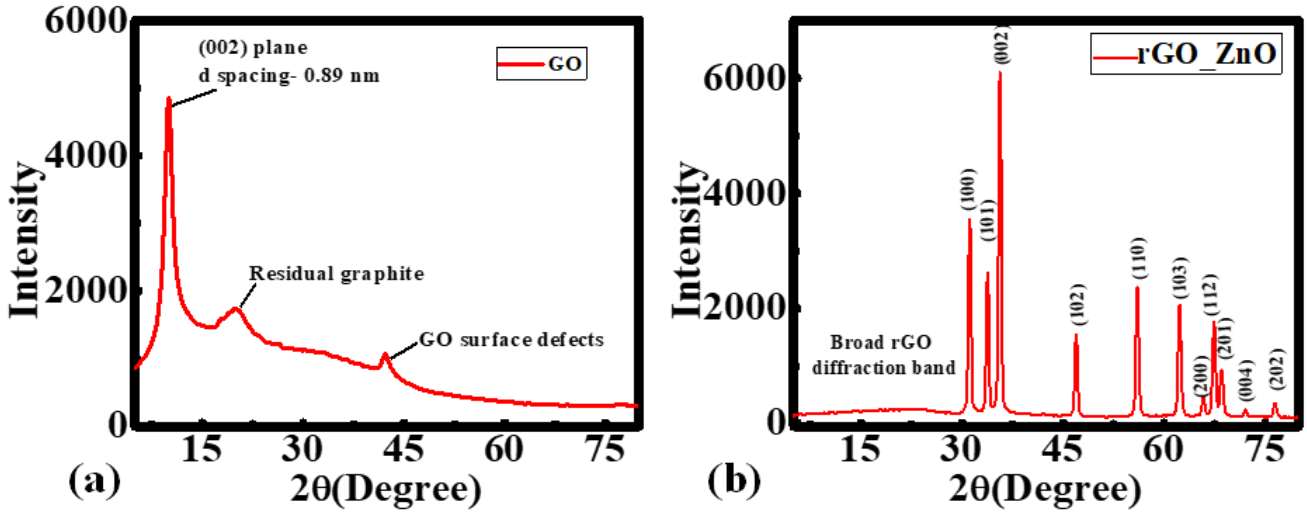

Fig 5.1: X-ray diffraction spectra of a) GO nanosheets and b) rGO_ZnO heterostructures.

X-ray diffraction spectra of GO nanosheets and rGO_ZnO heterostructures is presented in Fig 5.1. GO is characterized by a sharp (001) peak at around 2Θ=10.06º, which corresponds to the characteristic interlayer spacing of graphene oxide. [175] The lower value of 2Θ corresponds to a higher interlayer spacing which was measured to be 8.8 Å. This could be attributed to the modified value of $KMnO_4$ used in the reaction and a longer duration of the oxidation step which resulted in a large expansion of the graphene oxide sheets. The small peak around 21º could be attributed to the residual graphite or reduced GO formed due to the thermal reduction during the drying of the powder. The peak around 42º could be attributed to the surface defects in GO lattice. rGO_ZnO heterostructures show a broad, diffuse peak of rGO between 20-30 º with a negligible intensity compared to the crystalline ZnO phase. The presence of all the 11 characteristic peaks of ZnO- (100), (002), (101), (102), (110), (103), (002), (200), (112), (201), (004) and (202), between 30-80º [176] is an evidence of the excellent crystallinity which renders the heterostructures with remarkable functionality.

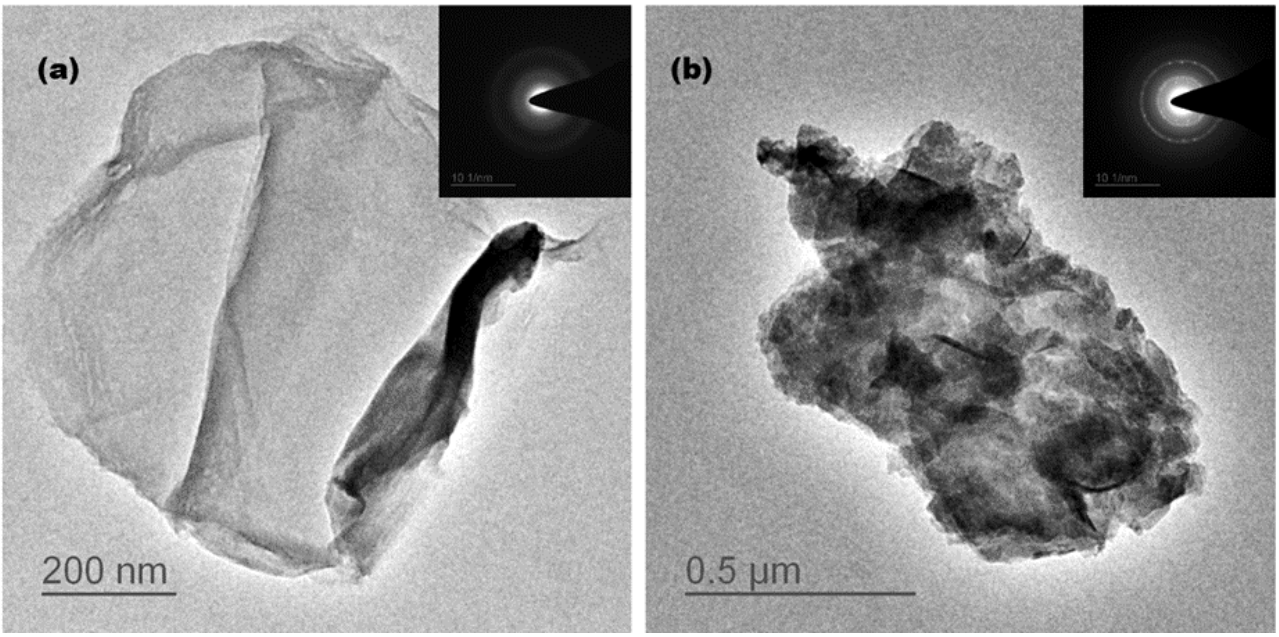

Fig 5.2: HRTEM images of a) GO nanosheets and b) rGO_ZnO heterostructures with SAED crystal structure data in inset.

Fig 5.2 depicts the TEM images and electron diffraction pattern of the synthesized nanomaterials. The HRTEM images of FLGO show 2-3 layers of graphene oxide stacked together, with each layer separated by a few nanometers. The high transparency obtained in the images is a characteristic feature of FLGO. The images also reveal the presence of defects on the edges of the sheet, which are created during the oxidation process. The wrinkled and crumpled morphology resembles to that of FESEM images. The HRTEM images of rGO_ZnO heterostructures show well-dispersed ZnO nanoclusters intercalated between the layers of rGO as depicted by the dark spots in the image. SAED was used to analyze the diffraction pattern of the materials. The diffraction pattern of FLGO shows highly diffuse rings, indicating a low degree of crystallinity. The diffraction pattern of rGO_ZnO heterostructures shows the diffraction spots of both rGO and ZnO, indicating the presence of both materials in the nanocomposite. The diffraction pattern of the ZnO nanoparticles was used to identify the crystal phase of ZnO. The d-spacing measured from the prominent rings represent the (100) and (101) planes which also correlates with the XRD data.

5.3.2 Morphological analysis

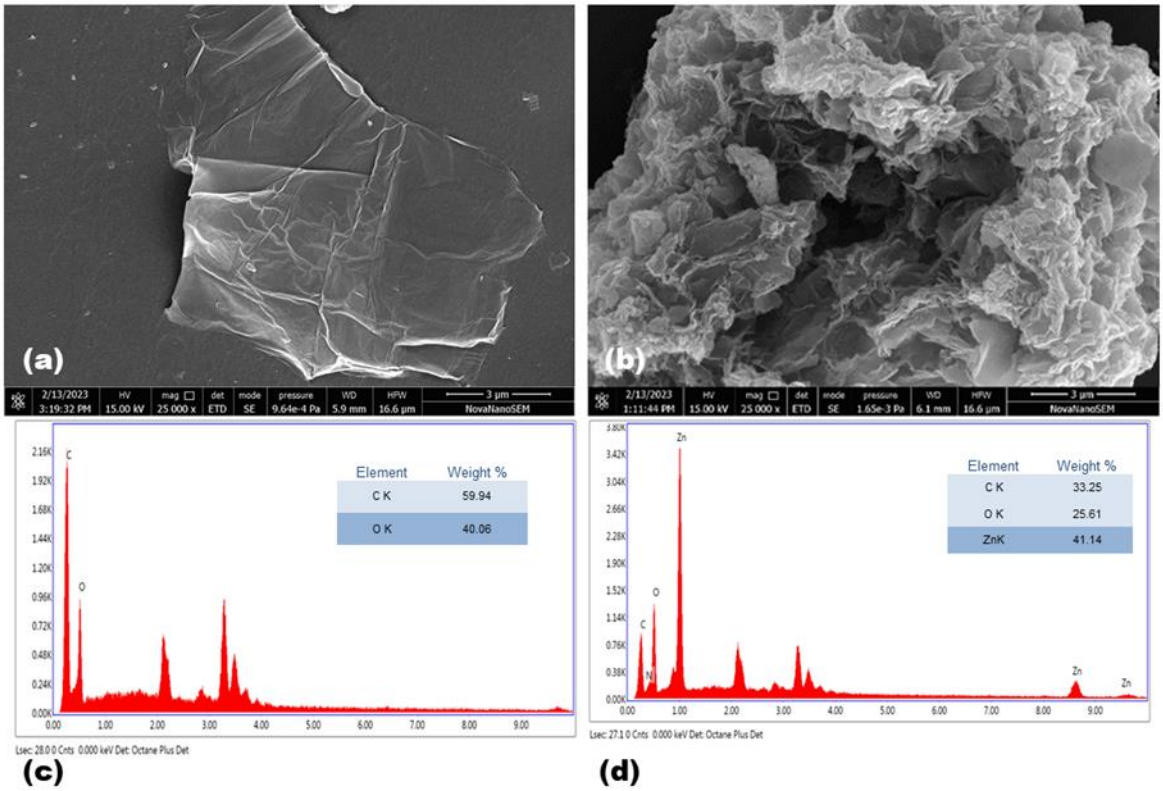

Fig 5.3: FESEM images of a) GO nanosheets and b) rGO_ZnO heterostructures. EDX spectra and elemental composition of c) GO nanosheets and d) rGO_ZnO heterostructures

Surface morphology and elemental composition of the nanopowders obtained from FESEM and EDX respectively is presented in Fig 5.3. The FESEM images illuminate the formation of Few-layer graphene oxide (FLGO) which is characterized by the presence of 2-3 layers of graphene oxide stacked together, with each layer separated by a few nanometers. The high resolution images of FLGO depict a typical crumpled structure, with wrinkles and folds on the surface of the material that are the result of the oxidation process, which causes the graphene layers to expand and become less stable. The surface of GO is typically covered with various types of oxygen-containing groups, such as hydroxyl, epoxy, and carboxyl groups, which renders it with the characteristic crumpled structure. The presence of few layers is evidence of an efficient oxidation and exfoliation process achieved during the synthesis. This could be attributed to the modified molar ratio of oxidizing agents compared to the conventional hummer's method and also to the longer duration of the oxidation step. In-situ synthesized

rGO_ZnO heterostructures are characterized by the presence of ZnO nanoclusters intercalated between the layers of reduced graphene oxide (rGO). The FESEM images of intercalated rGO_ZnO heterostructures show well-dispersed ZnO nanoclusters on the surface of the material, with a size range between 30-50 nm (also confirmed with AFM height profile). The composition of GO nanosheets and rGO_ZnO heterostructures is further confirmed with the EDX spectrum with the GO being consisting of 60% C and 40% O while the heterostructure confirms the presence of ZnO nanoparticles with 40 % Zn element. The O content significantly decreases in the heterostructure due to the removal of oxygen containing functional groups from the surface of GO nanosheets during the solvothermal reaction.

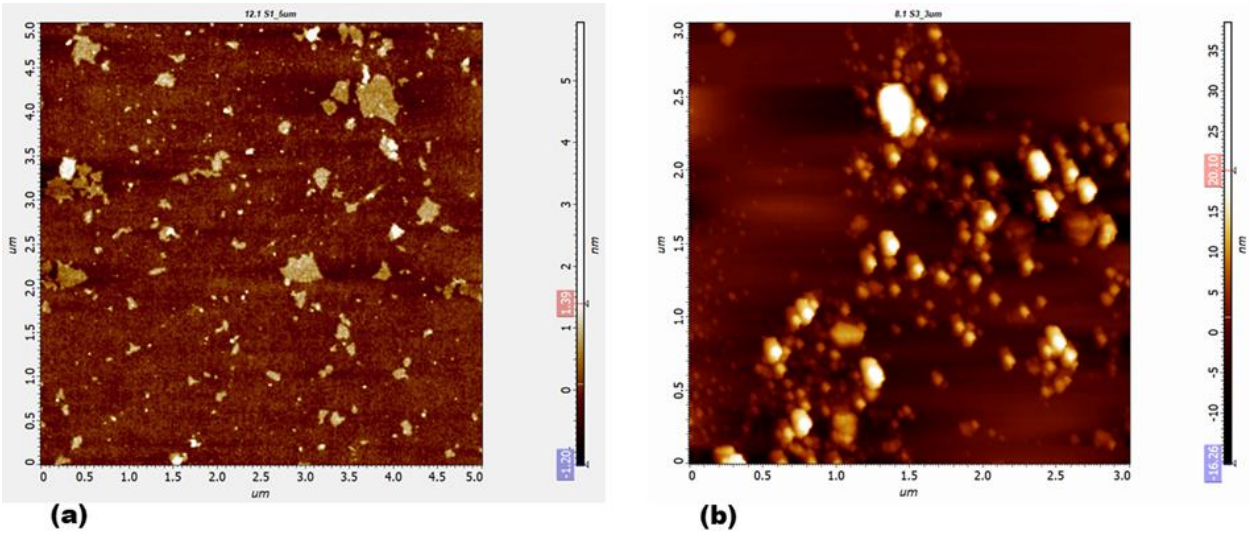

Fig 5.4: AFM surface topography images of a) GO nanosheets and b) rGO_ZnO heterostructures.

Surface topography profile of FLGO and rGO_ZnO heterostructure is presented in Fig 5.4- a and b respectively. The thickness of the graphene oxide nanosheets as measured from the AFM images ranges between 1.4-1.5 nm which confirms the formation of few layer graphene oxide since the interlayer spacing calculated from the XRD data was 0.89 nm. This observation is also in excellent agreement with the FESEM and HRTEM data and provides solid evidence of the efficient oxidation and exfoliation process. The rGO_ZnO heterostructures have an average height of approximately 30 nm due to the presence of intercalated ZnO nanoparticles between rGO nanosheets. The height profiles of both the nanomaterials are presented in Fig 5.5.

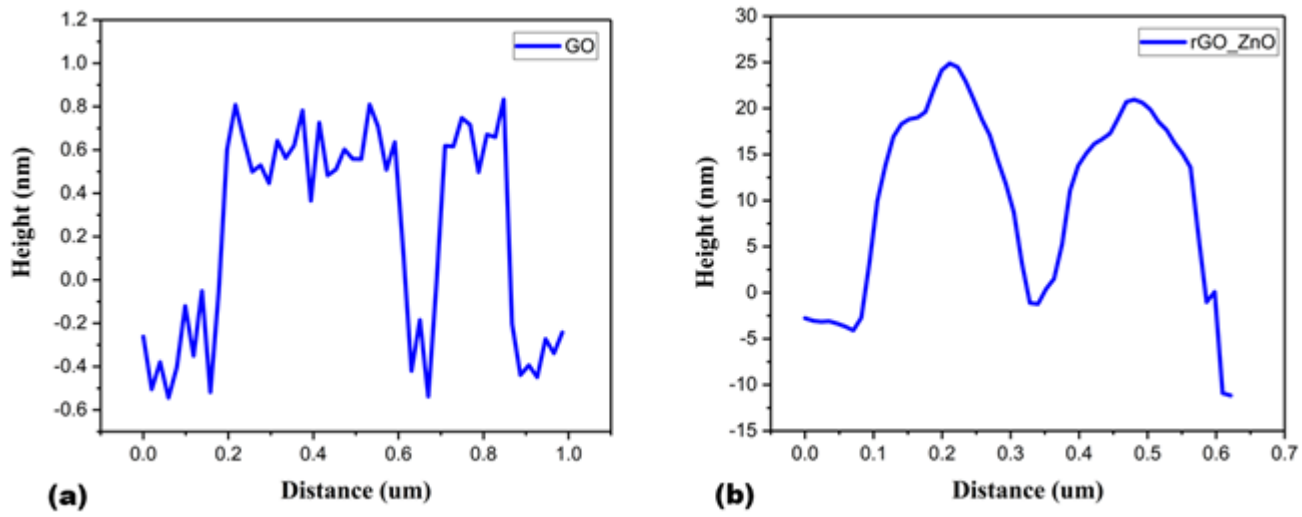

Fig 5.5: Thickness/Height profile derived from AFM topography of a) GO nanosheets and b) rGO_ZnO heterostructures.

5.3.3 Chemical analysis

FTIR spectra of GO nanosheets and rGO_ZnO heterostructures is presented in Fig 5.6. GO is characterized by strong absorption bands between 3100 cm-1 and 3400 cm-1, which corresponds to the stretching vibration of the hydroxyl (OH) and carboxyl (COOH) groups present on the surface of the material, a peak at around 1700 cm-1, corresponding to the stretching vibration of the C=O groups in the epoxy groups, the peak around 1648 cm-1 is attributed to C=C stretches from unoxidized graphitic domain, a peak at 2982 cm-1 corresponds to the stretching vibrations of the C-H group, 1228 cm-1 corresponding to C-OH stretch of alcohol group, and 1059 cm-1 is attributed to the C-O stretching vibrations of C-O-C [177]–[179]. rGO is characterized by a reduction in the intensity of the bands at 3100-3400 cm-1, 1228 cm-1, 1060 cm-1 and disappearance of the band at 1700 cm-1, which is attributed to the removal of the hydroxyl (OH) and carboxyl (COOH) groups present on the surface of the material. The appearance of a sharp peak at 1510 cm-1 is an evidence of the recovery of sp2 lattice of graphene. This observation is in excellent correlation with the PL emission peaks of rGO_ZnO heterostructures (Fig 5) which depict an increase in the sp2 hybridization. The rGO/ZnO heterostructures are characterized by an additional peak at around 460 cm-1, which corresponds to the characteristic Zn-O stretching vibration modes. [180]

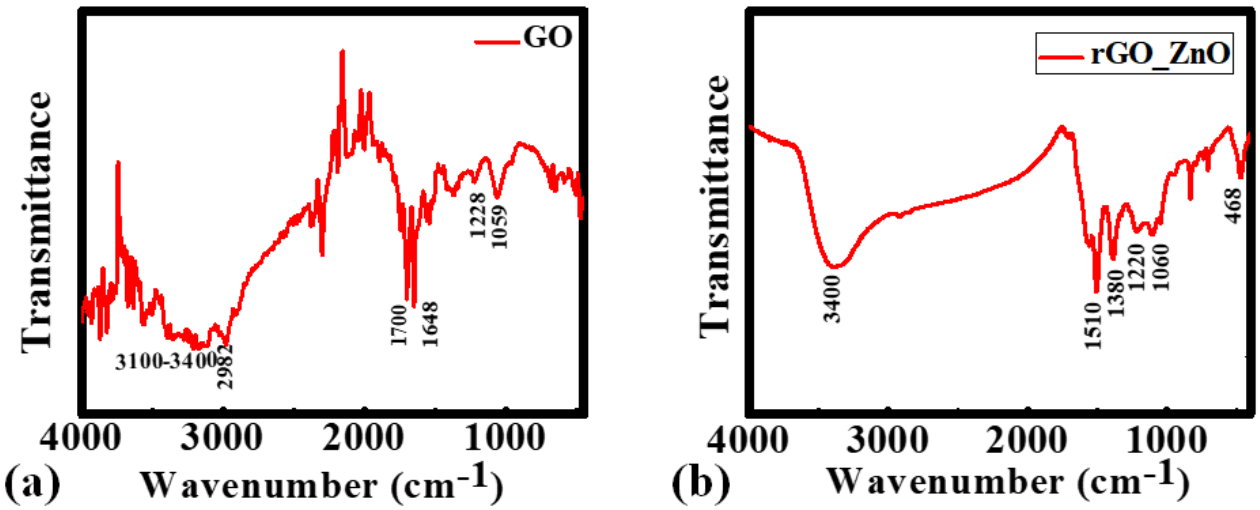

Fig 5.6: FTIR spectra of a) GO nanosheets and b) rGO_ZnO heterostructures in transmittance mode.

Raman spectra of GO nanosheets and rGO_ZnO heterostructures is presented in Fig 5.7. GO is characterized by a broad and intense D band at around 1352 cm-1, which is associated with the disorder and defects in the graphene lattice, and a weak and broad G band at around 1580 cm-1, which is associated with the E2g phonon mode of graphene. [181] The D band is representative of the sp3 bonded carbon atoms whereas the G band arises from the vibration of sp2 bonded carbon atoms. rGO is characterized by a sharp and intense G band at around 1580 cm-1, which is associated with the E2g phonon mode of graphene. The D band at around 1350 cm-1 becomes less intense and sharp as the degree of reduction increases, indicating a lower degree of disorder and defects in the graphene lattice. rGO_ZnO heterostructures are characterized by an additional peak at around 436 cm-1, which corresponds to the characteristic Raman E2 high mode of wurtzite hexagonal phase of ZnO. [182] A small bump at around 2900 cm-1, present in both the samples, is assigned to the D+G band. [183]

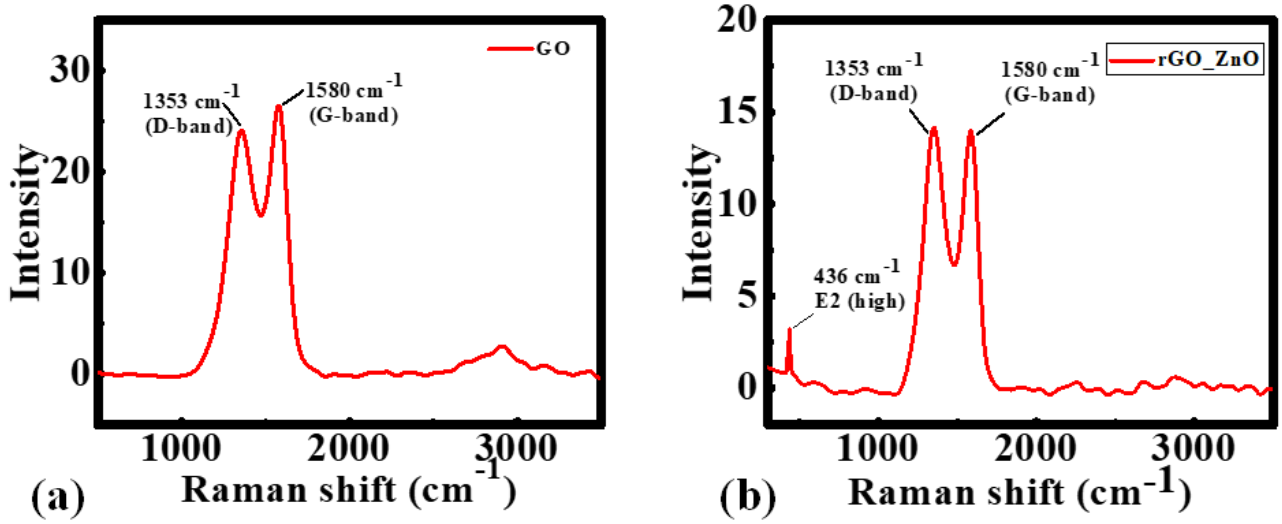

Fig 5.7: Raman spectra of a) GO nanosheets and b) rGO_ZnO heterostructures.

5.3.4 Optical analysis

UV-Vis spectra of nanopowders dispersed in DMF is presented in Fig 5.8. GO displays a single characteristic peak at 228 nm corresponding to the π-π^* transition.[184] The corresponding band energy was calculated using Tauc's method [135] assuming an indirect band gap for GO. (Fig 5.9) The absorption coefficient α is related to the band-gap energy E_g by the relation $(\alpha h\nu)^{\gamma} = A(h\nu - E_g)$ where ν is the photon frequency, A is a proportionality constant and γ denotes the nature of electronic transition having a value 1/2 for indirect band gap transitions and 2 for direct transitions. The band gap of GO nanosheets came out to be 2.24 eV. rGO_ZnO heterostructures display two

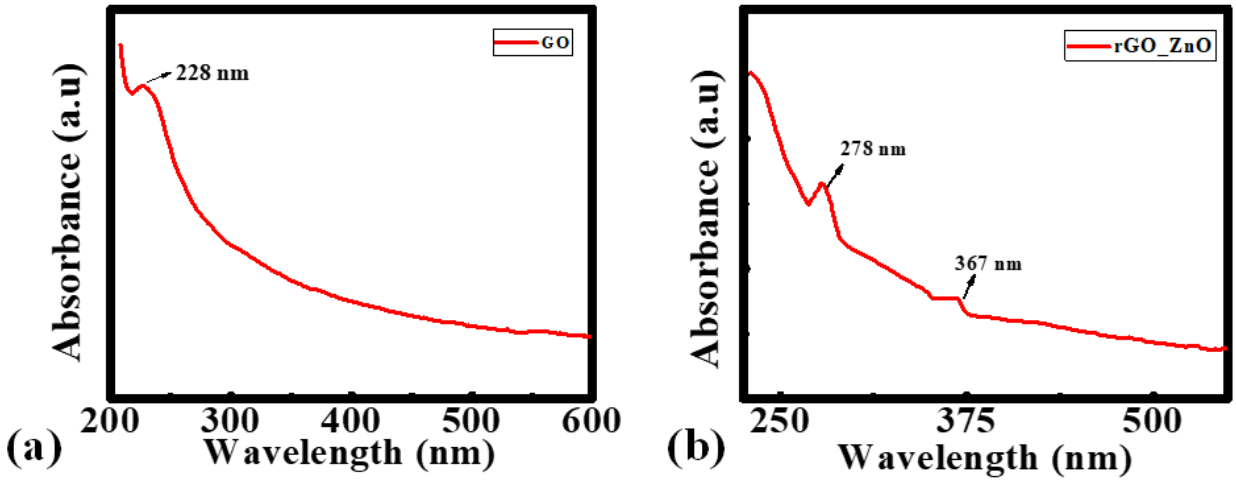

Fig 5.8: UV-Vis absorption spectra of a) GO nanosheets and b) rGO_ZnO heterostructures.

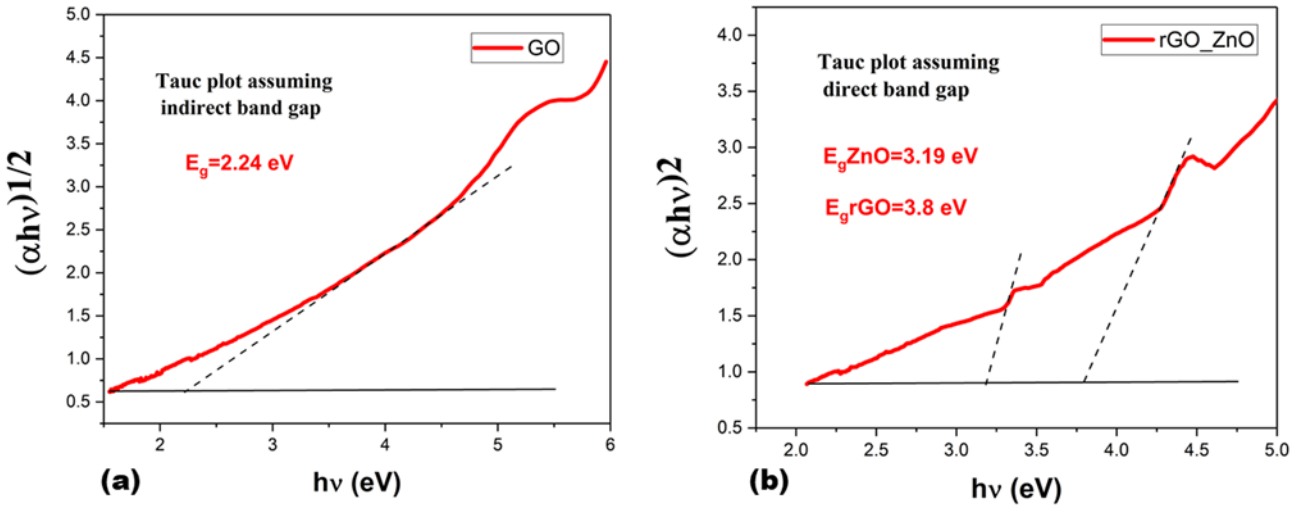

Fig 5.9: Tauc plot corresponding to UV-Vis absorption spectra of a) GO nanosheets and b) rGO_ZnO heterostructures.

peaks corresponding to both ZnO and rGO phase. The rGO peak is red shifted compared to the GO peak due to the removal of oxygen containing functional groups and is observed at 278 nm. The ZnO peak displays an absorption shoulder at 367 nm and is characteristic of the valence to conduction band transition. [185] The direct band gaps corresponding to the rGO and ZnO peak derived from the Tauc's plot came out to be 3.8 eV and 3.19 eV respectively. The wider band gap of the heterostructures compared to GO nanosheets enhances the charge trapping capabilities and consequently the electrical performance of the device.

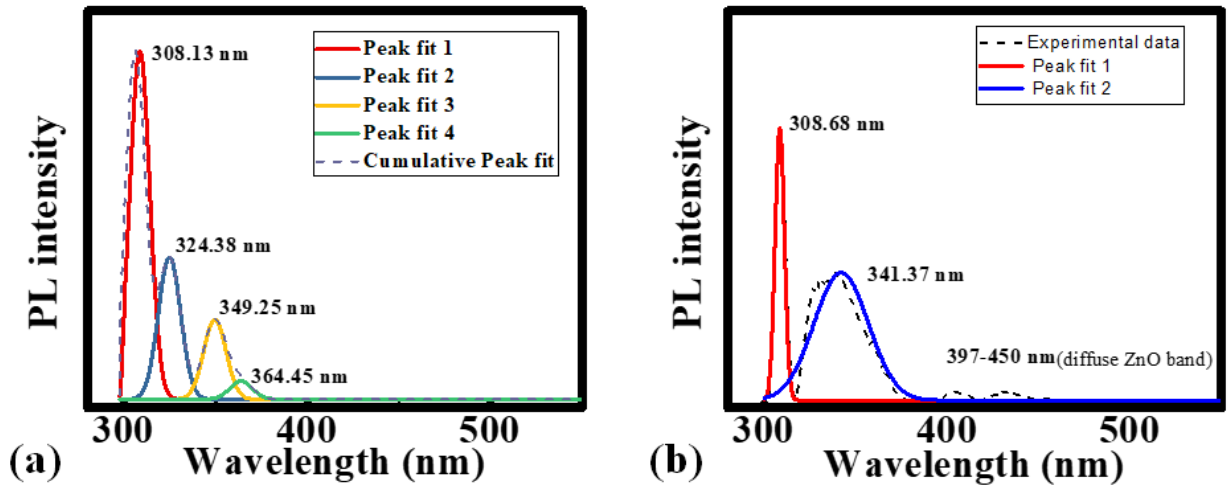

Fig 5.10: Deconvoluted PL emission spectra of a) GO nanosheets and b) rGO_ZnO heterostructures.

The photoluminescence emission spectra of the DMF dispersed nanopowders is presented in Fig 5.10. The PLE peaks were deconvoluted using Gaussian deconvolution and are presented along with cumulative peak data. Excitation wavelength used for the measurements was 280 nm. The PL curve of GO nanosheets was deconvoluted into 4 peaks at 308nm, 324nm, 349 nm and 365 nm corresponding to energies 4.02 eV, 3.83 eV, 3.55 eV and 3.39 eV respectively. The peaks at 4.02 eV and 3.83 eV are assigned to σ-σ^* transitions while the peaks 3.55 eV and 3.39 eV are assigned to π-π^* transition. [186] The PL spectrum of rGO_ZnO heterostructure displays two peaks corresponding to the rGO phase at 308nm and 341 nm with energies 4.02 eV and 3.6 eV. The 4.02 eV peak is assigned to the σ-σ^* transition although its intensity decreases as compared to the GO peak due to the decrease in density of states in σ-orbital caused by GO reduction. Simultaneously, the intensity of π-π^* transition peak (3.6 eV) in rGO increases in comparison to GO owing to the increase in density of states in π-orbital. These changes in the density states of σ and π orbital are related to the increase in sp2 hybridization due to the removal of oxygen containing functional groups from GO basal plane. The visible fluorescence of ZnO nanostructures is completely quenched in the rGO_ZnO heterostructures and only a diffuse emission band between 400-450 nm is observed. This observation is in agreement with the recent report by Chowdhury et al. who observed that the charge

recombination at oxygen vacancy in ZnO nanoparticles is suppressed by the charge transfer interactions with rGO nanosheets. [132]

5.4 Conclusion

GO was synthesized via modified Hummers method by oxidation of inexpensive graphite precursor with strong oxidising agents such as sulphuric acid and potassium permanganate with sodium nitrate as the catalyst. This synthesis was performed inside an ultrasonic bath to reduce the duration of oxidation step with faster exfoliation process that resulted in a decrease in the numbers of layers of GO. Solvothermal synthesis was utilized to prepare hybrid rGO/ZnO NP heterostructure. A comprehensive nanomaterial characterization utilizing advanced experimental techniques such as FESEM, HRTEM, AFM, RAMAN, PL, etc. was undertaken to study the structural, morphological, chemical, and optical properties of in-situ synthesized heterostructures. The presence of all the 11 characteristic peaks of ZnO in the XRD spectra provided evidence of the excellent crystallinity of the heterostructures. . The HRTEM images of FLGO show 2-3 layers of graphene oxide stacked together, with each layer separated by a few nanometers. The HRTEM images of rGO_ZnO heterostructures show well-dispersed ZnO nanoclusters intercalated between the layers of rGO. The FTIR and Raman spectra depicted an increase in the sp2 hybridization in rGO_ZnO heterostructures which was attributed to the recovery of graphene lattice owing to the removal of oxygen containing functional groups. The direct band gaps corresponding to the rGO and ZnO peak derived from the Tauc’s plot came out to be 3.8 eV and 3.19 eV respectively. The wider band gap of the heterostructures compared to GO nanosheets radically enhanced the charge trapping capabilities.